

Communications

The Solid Angle of a Plane Triangle

A. VAN OOSTEROM AND J. STRACKEE

Abstract—An analytical expression is presented for the solid angle subtended by a plane triangle at some arbitrary point in space. Using this expression, the time required for numerical computation is cut down to one third.

INTRODUCTION

One of the techniques commonly used for solving Neuman problems of potential theory leads to a formulation in which the potential Φ at some point inside the volume conductor can be found as a solution of an integral equation. When just a single interface bounding a homogeneous medium is involved, this equation reads

$$\Phi(Y) = G(Y) - \frac{1}{4\pi} \int_S \Phi(X) \frac{\mathbf{R} \cdot d\mathbf{S}}{R^3}. \quad (1)$$

In this formulation, $G(Y)$ is the potential at field point Y if the medium were homogeneous and of infinite extent, $\mathbf{R} = \mathbf{R}(Y, X)$ (norm R) is a vector pointing from surface point X to field point Y , and $d\mathbf{S} = d\mathbf{S}(X)$ is an element of the bounding surface S , directed along the local normal.

When the volume conductor is more complicated, i.e., involving multiple homogeneous regions of different electrical conductivity, the potential distribution can also be formulated in terms of integrals over the bounding surfaces (see Barnard *et al.* [1]). The same holds for the case when the problem involves Dirichlet boundary conditions in addition to Neuman conditions (see Barr *et al.* [2]).

When the shape of the bounding surface is complex, the solution of (1) can only be obtained numerically. The conversion of (1) into numerical form is obtained by representing the surface S by a large number of small plane triangles, the vertices of which lie on S . If the triangles are taken sufficiently small, the potential over each triangle Δ_j can be taken to be constant, say ϕ_j . Hence, the integral in (1) can be approximated by

$$\int_S \Phi \frac{\mathbf{R} \cdot d\mathbf{S}}{R^3} = \sum_{j=1}^N \phi_j \int_{\Delta_j} \frac{\mathbf{R} \cdot d\mathbf{S}}{R^3} \quad (2)$$

with N the total number of triangles.

The integral on the right-hand side of (2) can be recognized as being the solid angle ω_{ij} subtended by triangle Δ_j at field point Y_i (see, e.g., Barr *et al.* [2]).

Barnard *et al.* [1] have described a general expression for the computation of ω_{ij} . Using this expression, finding a single ω_{ij} involves 57 multiplications, 3 divisions, 40 additions/subtractions, and computing 3 square roots and 3 arctangents.

For the complete numerical treatment of (1) using the procedure as described by Barr *et al.* [3], the total number of

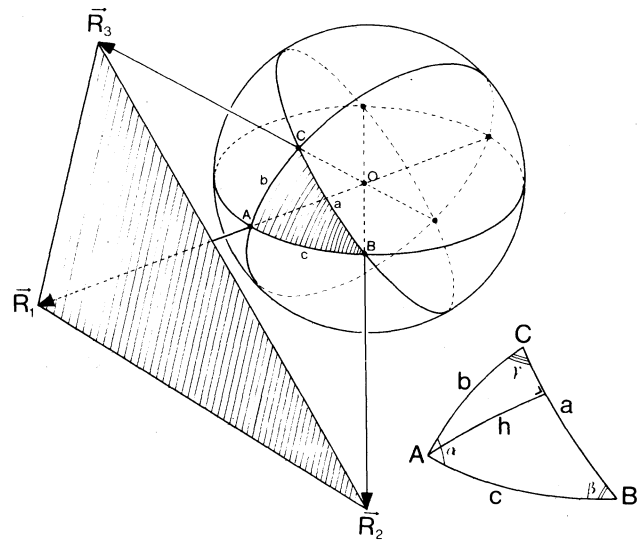


Fig. 1. Note: Characters with arrows appear boldface in text.

solid angles which have to be computed is $N \times K$, with K the number of vertices ($K = \frac{1}{2}N + 2$). For accurate results, K has to be large (> 100). Hence, the computation of all solid angles ω_{ij} requires a substantial amount of time.

The complexity of the expression for ω_{ij} as described by Barnard *et al.* [1] and the large number of computing steps make it rather sensitive to numerical errors, particularly so when the observation point is close to the triangle. In the next section, an expression is described in which the number of operations is cut down considerably, and which is far more transparent.

Note: The preceding was included to elucidate our interest in the solid angle computation. It is not meant to be a treatment of the numerical solution of potential problems.

THE SOLID ANGLE

Without loss of generality, the observation point can be placed at the origin. The three vertices of the plane triangle will be specified by the vectors \mathbf{R}_1 , \mathbf{R}_2 , and \mathbf{R}_3 ; see Fig. 1. By definition, the solid angle Ω subtended by this triangle at 0 is equal to S/r^2 , with S the area of the spherical triangle ABC of the sphere with radius r . Putting $r = 1$ implies that $\Omega = S$.

Under these conditions, the expression for Ω reads

$$\Omega = \alpha + \beta + \gamma - \pi, \quad (3)$$

a basic expression from spherical trigonometry in which α , β , and γ are the angles as indicated in Fig. 1.

Barnard *et al.* [1] have used this expression, backed by the following expression for α :

$$\alpha = \arctan \left(\frac{|(\mathbf{R}_3 \times \mathbf{R}_1) \times (\mathbf{R}_1 \times \mathbf{R}_2)|}{(\mathbf{R}_3 \times \mathbf{R}_1) \cdot (\mathbf{R}_1 \times \mathbf{R}_2)} \right) \quad (4)$$

and similar ones for β and γ found by cyclic permutations of the indexes. In a previous attempt to reduce the required computation time, we have used

$$\alpha = \arccos \left\{ \frac{|(\mathbf{R}_3 \times \mathbf{R}_1) \cdot (\mathbf{R}_1 \times \mathbf{R}_2)|}{|\mathbf{R}_3 \times \mathbf{R}_1| |\mathbf{R}_1 \times \mathbf{R}_2|} \right\}, \quad (5)$$

Manuscript received March 17, 1982; revised July 7, 1982.

A. van Oosterom was with the Laboratory of Medical Physics, University of Amsterdam, Amsterdam, The Netherlands. He is now with the Laboratory of Medical Physics and Biophysics, University of Nijmegen, Geert Groteplein Noord 21, 6525 EZ Nijmegen, The Netherlands.

J. Strackee is with the Laboratory of Medical Physics, University of Amsterdam, Amsterdam, The Netherlands.

which saved about 40 percent of computing time (van Oosterom [5]).

In a discussion of this problem, Dr. F. A. Muller of the Department of Physics of the University of Amsterdam pointed out that the numerical stability involved in (5) might be poorer than in (4). He also suggested that a more drastic reduction might be possible by considering the triple scalar product $\mathbf{R}_1 \cdot (\mathbf{R}_2 \times \mathbf{R}_3)$. While examining the various expressions for Ω alternative to (3) as described in (old) textbooks on spherical geometry, it became apparent how this advice could be put to use.

In Casey [4, result (359)], it is shown that

$$\cos\left(\frac{1}{2}\Omega\right) = \frac{1 + \cos(a) + \cos(b) + \cos(c)}{4 \cos\left(\frac{1}{2}a\right) \cos\left(\frac{1}{2}b\right) \cos\left(\frac{1}{2}c\right)}, \quad (6)$$

with a , b , and c the arcs among A , B , and C as indicated in Fig. 1. This can be noted as

$$\cos\left(\frac{1}{2}\Omega\right) = \frac{1 + \sum_i \cos(x_i)}{4 \prod_i \cos\left(\frac{1}{2}x_i\right)},$$

$i = 1, 3, x_1 = a, x_2 = b, x_3 = c.$

By using the basic trigonometric relationships

$$\cos^2\left(\frac{1}{2}x\right) = \frac{1}{2} \{ \cos(x) + 1 \}$$

and

$$\tan^2\left(\frac{1}{2}\Omega\right) = \frac{1}{\cos^2\left(\frac{1}{2}\Omega\right)} - 1,$$

it can be easily verified that

$$\tan\left(\frac{1}{2}\Omega\right) = \frac{\left\{ 1 + 2 \prod_i \cos(x_i) - \sum_i \cos^2(x_i) \right\}^{1/2}}{1 + \sum_i \cos(x_i)}. \quad (7)$$

The numerator in this expression is equal to $\sin(a) \sin(h)$, with h the arc between A and its spherical projection onto BC (see Casey [4, results (44) and (57)]). From the geometrical interpretation of the triple scalar product $[\mathbf{R}_1 \mathbf{R}_2 \mathbf{R}_3] = \mathbf{R}_1 \cdot (\mathbf{R}_2 \times \mathbf{R}_3)$, i.e., the volume of the parallelepiped spanned by the vectors \mathbf{R}_1 , \mathbf{R}_2 , and \mathbf{R}_3 , it follows that $[\mathbf{R}_1 \mathbf{R}_2 \mathbf{R}_3] = R_1 R_2 R_3 \sin(a) \sin(h)$. Hence, multiplying the numerator and denominator of (7) by $R_1 R_2 R_3$ and using the property of the scalar product $\mathbf{R}_i \cdot \mathbf{R}_j = R_i R_j \cos(\mathbf{R}_i \mathbf{R}_j)$ results in

$$\tan\left(\frac{1}{2}\Omega\right) = \frac{[\mathbf{R}_1 \mathbf{R}_2 \mathbf{R}_3]}{R_1 R_2 R_3 + (\mathbf{R}_1 \cdot \mathbf{R}_2) R_3 + (\mathbf{R}_1 \cdot \mathbf{R}_3) R_2 + (\mathbf{R}_2 \cdot \mathbf{R}_3) R_1}. \quad (8)$$

By using the Fortran function ATAN2,

$$\Omega = 2 * \text{ATAN2}(N, D),$$

with N and D the numerator and denominator of (8), the ordering of \mathbf{R}_1 , \mathbf{R}_2 , and \mathbf{R}_3 automatically leads to a change in sign when the observation point moves from one side of the plane of the triangle to the other side. In contradistinction, the method of Barnard *et al.* requires the additional computation of the normal to the plane triangle to establish the correct sign.

The computation involves 32 multiplications, 20 additions, 3 square roots, and 1 ATAN2.

REFERENCES

- [1] A.C.L. Barnard, I. M. Duck, M. S. Lynn, and W. P. Timlake, "The application of electromagnetic theory to electrocardiology II," *Biophys. J.*, vol. 7, pp. 463-491, 1967.
- [2] R. C. Barr, T. C. Pilkington, J. P. Boineau, and M. S. Spach, "Determining surface potentials from current dipoles with application to electrocardiography," *IEEE Trans. Biomed. Eng.*, vol. BME-13, pp. 88-92, Apr. 1966.
- [3] R. C. Barr, M. Ramsey, and M. S. Spach, "Relating epicardial to body surface potential distributions by means of transfer coefficients based on geometry measurements," *IEEE Trans. Biomed. Eng.*, vol. BME-24, pp. 1-11, Jan. 1977.
- [4] J. Casey, *A Treatise on Spherical Trigonometry*. Dublin, Ireland: Hodges, Figgis & Co., 1889.
- [5] A. van Oosterom, "Cardiac potential distributions," thesis, Univ. Amsterdam, Amsterdam, The Netherlands, 1978.

A Simple Computerized Neuroanatomical Data Collection System

A. VANIA APKARIAN, CHARLES J. HODGE, H. JAY WISNICKI,
AND JONATHAN DELATIZKY

Abstract—A semiautomated data collection system, flexible enough to apply to any microscopic tissue where the data can be accepted as point positions, is described. The design is simple and can be easily implemented on a mini- or microcomputer with minimal additional hardware. The results of a typical neuroanatomical experiment are shown together with an error and time constraint analysis.

INTRODUCTION

The nature of neuroanatomical data poses difficulties in creating permanent records that can be collected in a reasonable amount of time, occupy a minimal amount of space, and be recalled easily for further analysis. Currently, a number of research groups [2], [4], [5], [10]-[12], [14], [19], [20], [24], [25], [27], [28], [30], [32]-[34] possess automated or semiautomated data collection systems. The success of these systems is linked to the neuroanatomical techniques used. Autoradiography lends itself to quantitative analysis, where single granules can be counted over a given field of nervous tissue rapidly and accurately with minimal human intervention [32], [34]. The analysis of golgi-stained tissue requires systems capable of tracking neuronal processes in three dimensions at a high resolution [3], [11], [12], [20], [25], [30], [33], [34]. Other techniques are limited by subjective identification of the presence of a specific label, where

the judgment of an operator is indispensable. Retrograde labeling of neurons by horseradish peroxidase [16], [18], glyoxylic acid induced fluorescence of noradrenaline containing cells or terminals [7], and the Falck-Hillarp [8], [9] technique to induce fluorescence in catecholamine or serotonin containing regions in the brain or spinal cord are examples of methods where introduction of automated techniques has

Manuscript received October 1, 1980; revised August 11, 1982. This work was supported in part by the NINCDS under Grant 5R01NS1276103.

The authors are with the Upstate Medical Center, Syracuse, NY 13210.